RESEARCH ARTICLE

WILEY SURFACE and INTERFACE ANALYSIS

The interface electrochemical and chemical mechanism of a low alloy steel in a 3.5% NaCl solution containing Ce^{3+}-based inhibitor

Xingyue Yong[1] (ID) | Zhenning Chen[1] | Jinjie Pan[1] | Yanna Teng[1] | Ying Wang[1] | Zhenxing Feng[2]

[1] State Key Laboratory of Organic-Inorganic Composites, Beijing University of Chemical Technology, Beijing 100029, China

[2] School of Chemical, Biological, and Environmental Engineering, Oregon State University, Corvallis, OR 97331, USA

Correspondence
Xingyue Yong, Beijing University of Chemical Technology, Beijing 100029, China.
Email: yongxy@mail.buct.edu.cn

The interface electrochemical and chemical mechanism of the low alloy steel in a 3.5% NaCl solution containing the Ce^{3+}-based inhibitor was investigated by the electrochemical techniques in conjunction with the surface analysis technologies. It was shown that the Ce^{3+}-based inhibitor was an anodic inhibitor with more than 90.0% inhibitory efficiency. The net-shaped inhibiting film with 200 to 500-nm greyish balls was observed on the specimen surface. During the corrosion reaction occurred on the surface of the low alloy steel, the hydrolysis reaction of $P_3O_{10}^{5-}$ and the disproportionation reaction of Ce^{3+} ions simultaneously occurred, too, resulting in the formation of the net-shaped inhibiting film with nano-scale greyish ball-type products, which contained Ce element and had an obvious effect on the electrochemical process of the low alloy steel in a 3.5% NaCl solution containing the Ce^{3+}-based inhibitor. Therefore, the EIS spectra of the low alloy steel in a 3.5% NaCl solution containing the Ce^{3+}-based inhibitor were composed of a capacitive loop at a high-frequency region and an inductive impedance loop at a low-frequency region. The charge-transfer resistance (R_t) increased with the immersion elapsed time, indicating that the inhibition efficiency of the Ce^{3+}-based inhibitor increased with immersion elapsed time. The calculated data based on the fitted electrochemical parameters showed the partial coverage of the inhibitor. This was further revealed by the analysis of electrochemical kinetics that the inductive impedance (L) loop at a low frequency region resulted from the localized absorption of the Ce^{3+}-based inhibitor on the surface of the low alloy steel in a 3.5% NaCl solution. It was also verified by micro-morphologies.

KEYWORDS

Ce^{3+}-based inhibitor, electrochemical technique, interface mechanism, low alloy steel, NaCl solution, surface analysis

1 | INTRODUCTION

As the increasing applications of steel-based materials in diverse ocean conditions, the steel structures are subjected to serious corrosion in seawater. Therefore, several methods such as organic coatings and cathodic protection have been used to protect the steel structures.[1] Among these strategies, the application of inhibitors is regarded as an economic and effective way in industrial fields.[2] In past years, researches were mainly focused on the usages of the inhibitors for carbon steel in water.[3-5] There are few inhibitors available for low alloy steels in a chloride solution or seawater. However, some highly effective inhibitors are required for the application of low alloy steel in ocean industry.

Recently, the applications of rare earth elements (Re) have caught the attention of corrosion scientists.[6-12] For example, cerium chloride ($CeCl_3$) not only acted predominantly as a mixed inhibitor for carbon steel in natural seawater,[13] but also the inhibitor ($Ce(NO_3)_3 + Na_2MoO_4$) had a better inhibition effect for X70 steel in a 3.5 NaCl solution.[14] Ce^{3+} was also used as 1 component of the inhibitor for protecting AA3003 aluminum alloy from corrosion in the flowing ethylene glycol-water solution.[15] In addition, $CeCl_3$ was still tested as the inhibitors for AA2204-T3 and AA5083 aluminum alloys

in a chloride solution.[16-19] Although the rare earth elements, which act as 1 component of an inhibitor, show great effects in corrosion protection, little has been known for the interface electrochemical and chemical mechanism of Ce^{3+}-based inhibitors for low alloy steels in chloride solutions. In particular, the studies on the electrochemical kinetic process of low alloy steels in a corrosive media containing Re-based inhibitors are rare. This hampers the developments and applications of some highly effective Re-based inhibitors in industrial fields.

In this work, the interface electrochemical and chemical mechanism of the low alloy steel in a 3.5% NaCl solution containing the Ce^{3+}-based inhibitor was investigated by electrochemical techniques in conjunction with surface analysis technologies to understand the inhibitory mechanism of the Ce^{3+}-based inhibitor. Our results will provide first clear insights into the interface electrochemical and chemical mechanism of the Re-based inhibitor to protect the low alloy steel in a chloride solution from corrosion.

2 | MATERIALS AND EXPERIMENTAL METHODS

The material used in this study was the low alloy steel (wt.%: C, 0.073; Si, 0.29; Mn, 0.43; S, 0.0044; P, 0.010; Cr, 1.02; Ni, 2.65; Mo, 0.26; V, 0.058; Fe, balance). All specimens were wet polished with SiC paper up to 800 grit and then cleaned using the ultrasonic method, degreased with ethanol, and finally dried in desiccators. The inhibiting efficiency was determined by weight loss. Specimens were weighed by electronic analytical balance with 0.1-mg precision.

The test media, which were a 3.5% NaCl solution, were prepared by dissolving 35.0 g of NaCl in 1.0-L top water. Before experiments, the test media were left without stirring to a room temperature in contact with air.

Both electrochemical polarization and EIS spectra of the electrodes made of the low alloy steel in a 3.5% NaCl solution without and with the Ce^{3+}-based inhibitor for different immersion time were conducted using an electrochemical test system with a 3-electrode test cell, and the specimens were used as working electrodes. Saturated calomel electrodes and platinum wire were used as reference electrodes and counter, respectively. Potentiodynamic polarization curves were measured at the potential sweep rate of 1 mV/s. EIS spectra were measured at a small sinusoidal voltage perturbation (±5 mV) over a range of frequencies from 100 kHz to 0.01 Hz and were fitted with Gamry Echem Analyst software using Simplex method in accordance with the equivalent electric circuit. The goodness of fitting is below 1.0×10^{-4}.

The corroded surface morphologies were observed by scanning electric microscope (SEM) (Muitimode III a, US DI Co., Ltd), and the elemental compositions of the inhibitory film were analyzed with EDX technology. At the same time, atomic force microscope (AFM) was used to further analyze the corroded surface morphologies. The chemical compositions of the inhibitory film on the specimen surface were investigated using X-ray photoelectron spectroscopy (XPS) and were performed using an ESCALAB 250 instrument with a monochromatic Al-Kα radiation source. Fitting curves was performed using the commercial XPS peak version 4.1 software.

3 | RESULTS AND DISCUSSION

3.1 | Characterization of the inhibitory film

3.1.1 | Morphological features

Based on the studies on the inhibitory efficiencies of some chemical agents to a low alloy steel in a 3.5% NaCl solution, the Ce^{3+}-based inhibitor formulation (40 ppm $CeCl_3$ + 20 ppm $NaNO_2$ + 300 ppm $Na_5P_3O_{10}$) was determined by weight loss in the conjunction with the orthogonal experimental design. Figure 1 shows their surface morphologies after specimens were immersed in a 3.5% NaCl solution without and with the Ce^{3+}-based inhibitor, respectively. As shown in Figure 1A, the tested specimen surface was partially covered with brown rust products, and the polish traces became vague, showing the tested specimen suffered from serious corrosion in a 3.5% NaCl solution. However, once the inhibitor was added to a 3.5% NaCl solution, the specimen surface was covered with a net-shape film with greyish products, most of which had a small size, and the polish traces were clearly observed (Figure 1B), indicating that the Ce^{3+}-based inhibitor was used to retard the corrosion of the specimen, and that it was found that its inhibitory efficiency was more than 90.0%.

To further observe the morphology of the inhibiting film formed on the surface of the specimen, its AFM images were presented in Figure 2 before immersion and after the specimen had been immersed in a 3.5% NaCl solution containing the Ce^{3+}-based inhibitor for 30.0 hours. As shown in phase image depicted in Figure 2A-1 and A-
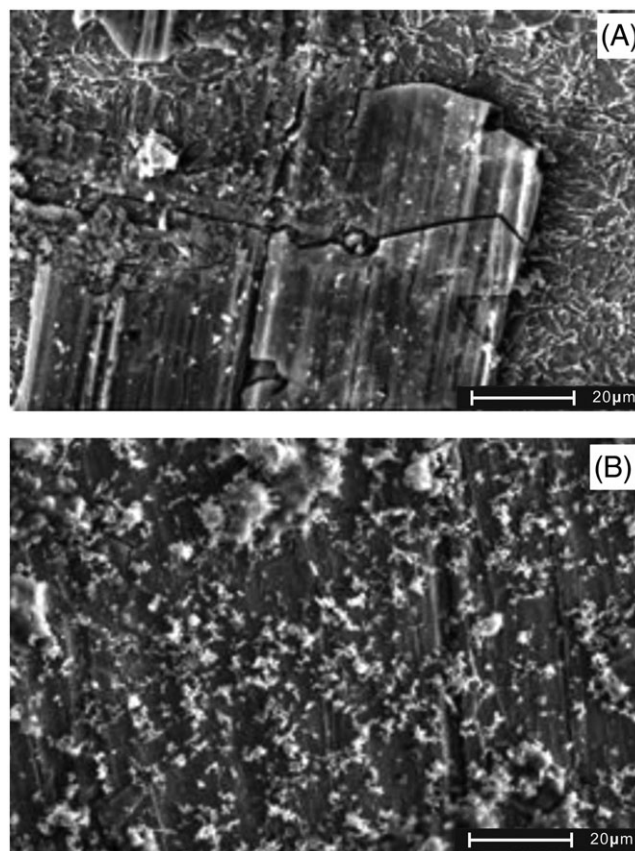

FIGURE 1 SEM images of the corroded surfaces of specimens (A, in a 3.5% NaCl solution; B, in a 3.5% NaCl solution containing the Ce^{3+}-based inhibitor)
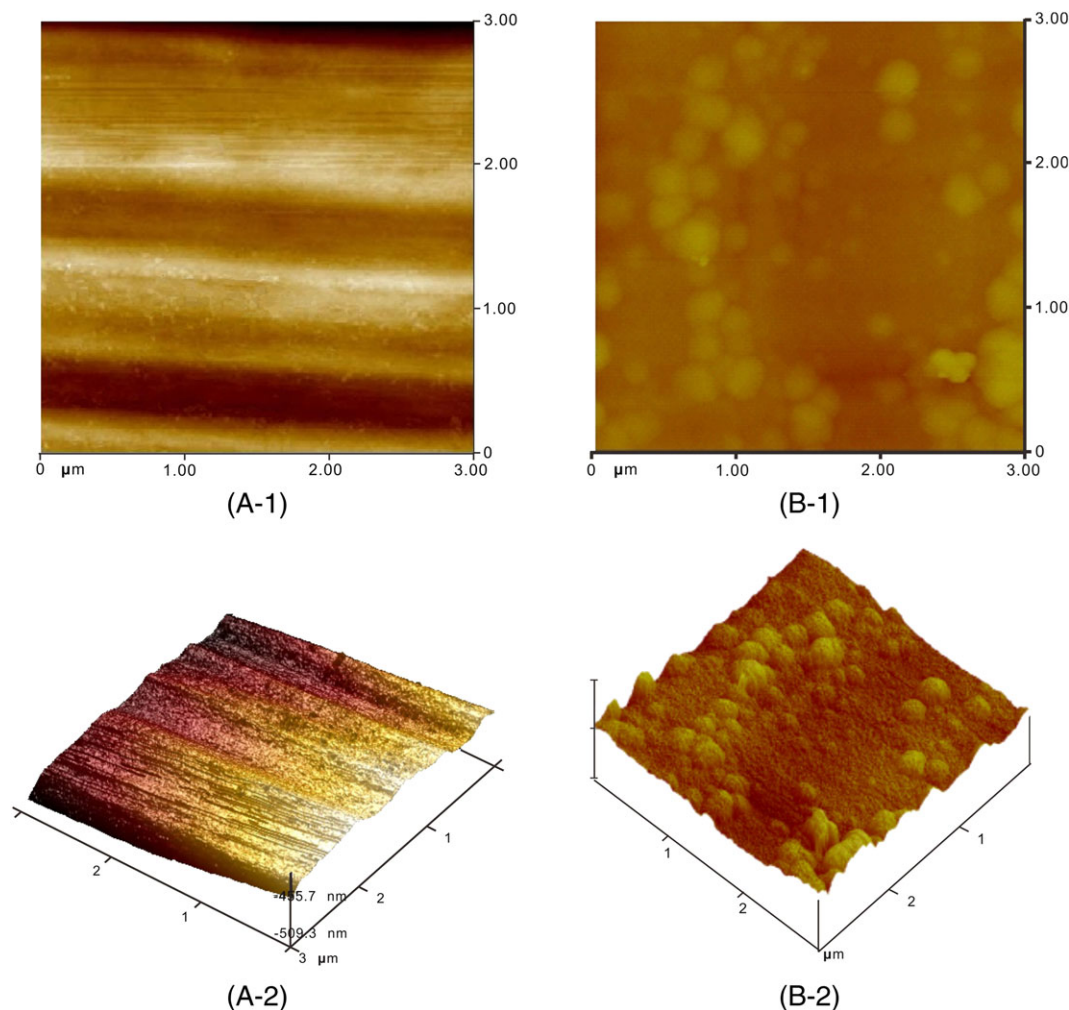
FIGURE 2 AFM images of specimen before immersion and after immersed for 30 hours in a 3.5% NaCl solution containing the Ce^{3+}-based inhibitor (A, as-received, B, after test; A-1, B-1: Phase image; A-2, B-2: Height image)

2, the surface of the as-received specimen was very clean and was covered with very small polish traces. However, after the specimen had been tested for 30.0 hours, it was found that there were some greyish ball-type particles on the surface of the specimen (Figure 2B-1), and that the inhibiting film was composed of towering ball-type particles and smooth dark film (Figure 2B-2), the sizes of greyish ball-type particles were 200 to 500 nm, further indicating that the inhibitory film was a kind of net-type inhibiting film with nano-scale greyish ball-type products.

3.1.2 | Chemical compositions of the inhibitory film

In this work, EDX technology was used to study the elemental compositions of the inhibitory film. The EDX spectra were shown in Figure 3.

It was found in Figure 3A that the greyish products on the specimen surface mainly contained O, Na, Fe, P, Ce, and Ca elements. The balance surface without the coverage of greyish products mainly contained O, Ni, Cr, Fe, P, Ce, and Ca elements, see Figure 3B. By comparison, greyish products involved much more O, Na, P, Ce, and Ca elements and did not contain Ni and Cr elements, indicating that the greyish products would be composed of the phosphates of Na, Fe, Ce, and Ca elements containing a few of Fe and Ce oxides. The balance

surface would mainly be covered with Fe, Ni, Cr, and Ce oxides containing a few of Na and Ca phosphates.

At the same time, the specimen surface was analyzed with XPS technology. The XPS spectra were shown in Figure 4A. Based on Figure 4A, the valence states of P and Ce elements were further analyzed using the commercial XPS peak version 4.1 software. The fitting curves were shown in Figure 4B,C. It can be seen from Figure 4B that the inhibitory film contained 16.8% PO_4^{3-} and 83.2% $P_2O_7^{4-}$, respectively. It was indicated that $Na_5P_3O_{10}$ in a 3.5% NaCl solution transferred into PO_4^{3-} and $P_2O_7^{4-}$ due to the hydrolysis of $Na_5P_3O_{10}$ compound. On the other hand, it was found in Figure 4C that the inhibitory film contained 40.0% Ce^{2+}, 58.0% Ce^{3+}, and 2.0% Ce^{4+}, respectively. It was shown that both oxidized and reductive reactions occurred to Ce^{3+} under the actions of resolved oxygen and NO_2^-. Therefore, Ce^{3+} simultaneously transferred into Ce^{2+} and Ce^{4+}.

3.2 | Effect of the inhibitory film

To study the effect of the inhibitory film containing Ce element on the electrochemical polarization behavior of the low alloy steel in a 3.5% NaCl solution, the polarization curves were performed, and the results were shown in Figure 5.
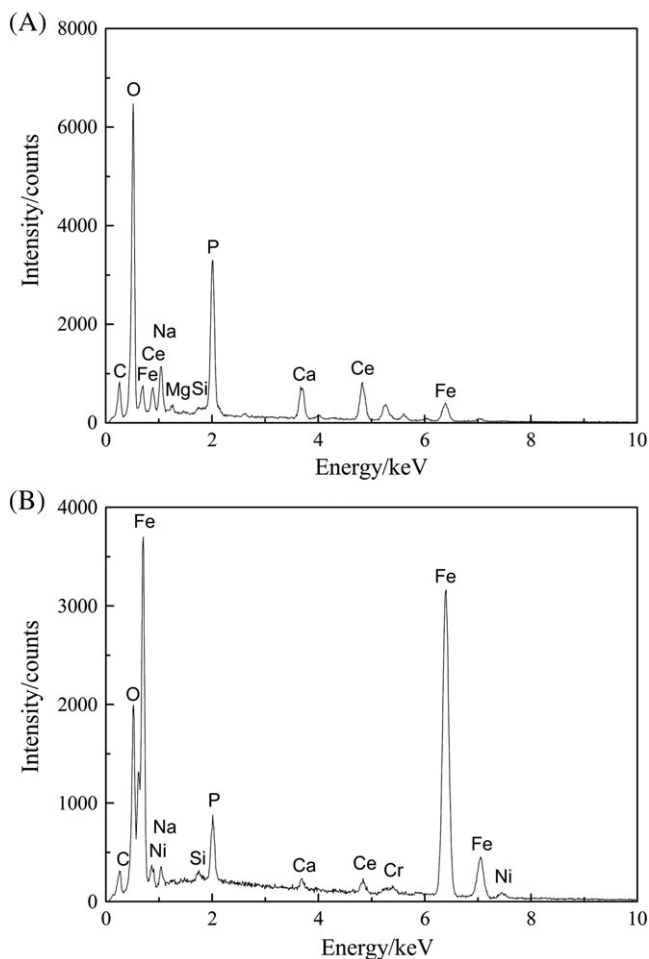
FIGURE 3 EDX spectra of the inhibitory film (A, the greyish products on the specimen surface; B, the balance surface without the coverage of greyish products)

Figure 5 shows that the anodic process of the low alloy steel in a 3.5% NaCl solution was active, and the cathodic process was controlled by oxygen diffusion. Therefore, corrosion process of the low alloy steel in a 3.5% NaCl solution was controlled by oxygen diffusion. Once the Ce^{3+}-based inhibitor was added to a 3.5% NaCl solution, its corrosion potential became more positive due to the formation of the inhibitory film containing Ce element on the surface of the low alloy steel. In this case, the anodic process exhibited passive behavior, and the anodic coefficient of the Ce^{3+}-based inhibitor ($(f_a)_{-0.5\ V}$):

$$(f_a)_{-0.5\ V} = \left(\frac{I'_a}{I_a}\right)_{-0.5V} = 0.014.$$ The cathodic process was still controlled by oxygen diffusion, and the cathodic coefficient of the Ce^{3+}-based inhibitor ($(f_c)_{-0.8\ V}$): $(f_c)_{-0.8\ V} = \left(\frac{I'_c}{I_c}\right)_{-0.8V} = 1.49$. Therefore, $(f_a)_{-0.5\ V} \ll (f_c)_{-0.8\ V}$, where I_a and I'_a are the anodic current density of electrode in a 3.5% NaCl solution without and with the inhibitor at the same anodic polarization potential, respectively; I_c and I'_c are the cathodic current density of electrode in a 3.5% NaCl solution without and with the inhibitor at the same cathodic polarization potential, respectively. It was shown that the inhibiting effect to the anodic process was higher than that to the cathodic process.[20] The
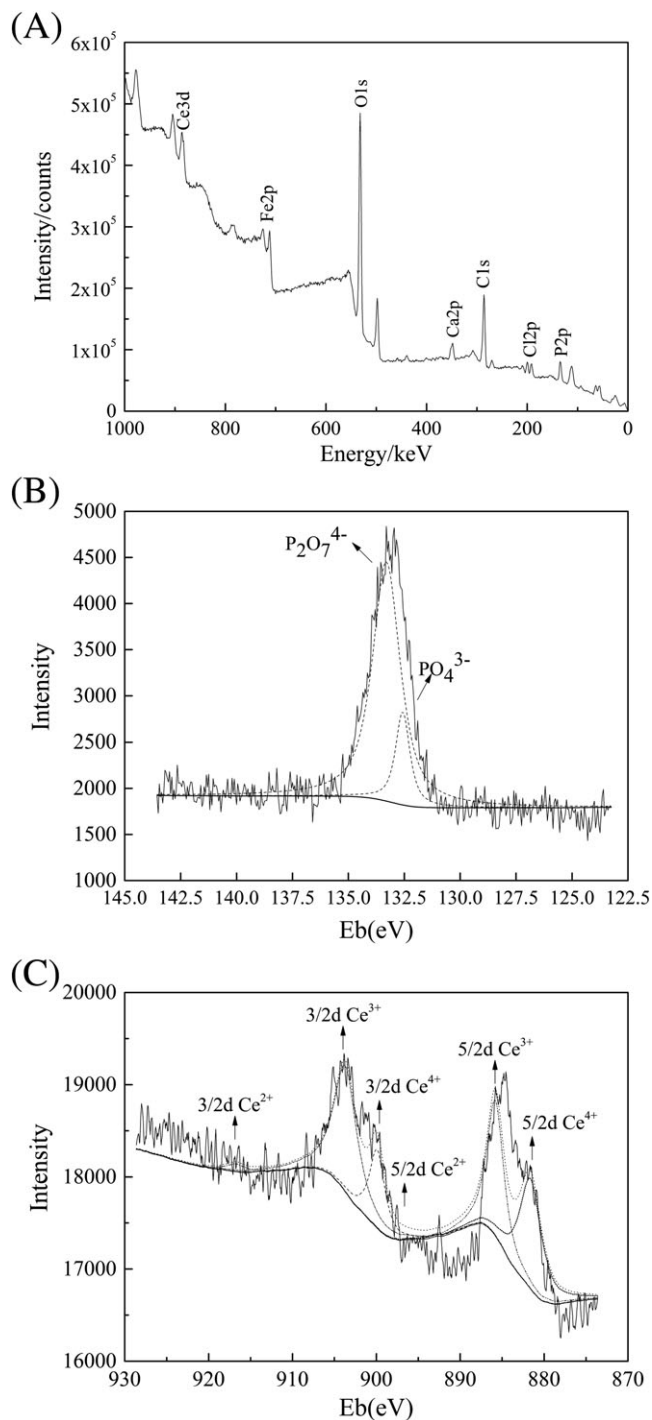

FIGURE 4 XPS spectra of the inhibitory film (A, XPS spectra of P and Ce elements in the inhibitory film; B, P 2P XPS spectra; C, Ce $\frac{5}{2}$P and 2P XPS spectra)

corrosion of the low alloy steel was obviously controlled by anodic passivation process. The Ce^{3+}-based inhibitor was an anodic inhibitor.

3.3 | Characteristics of interface electrochemical reaction

3.3.1 | EIS spectra

The electrochemical impedance spectroscopy (EIS) is a powerful tool for studying the electrochemical kinetic process of metals in corrosive media.[21,22]
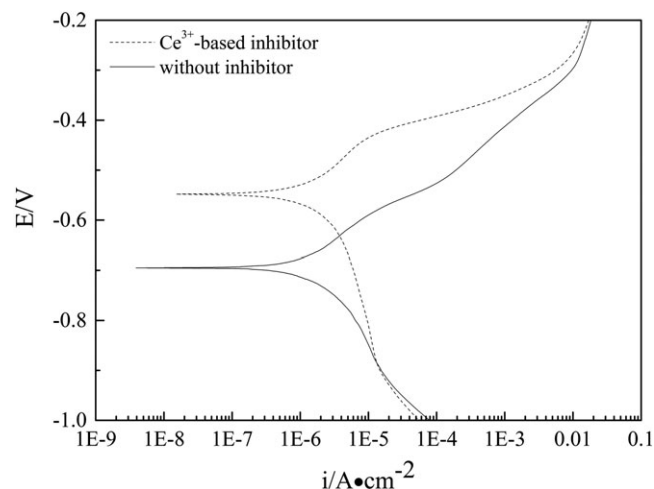
FIGURE 5 Polarization curves of the low alloy steel in a 3.5% NaCl solution without and with the Ce^{3+}-based inhibitor

To further understand the interface electrochemical kinetics between the steel surface and corrosive media, the EIS spectra of the low alloy steel in a 3.5% NaCl solution without and with the inhibitor were performed.

As shown in Figure 6, EIS spectra were composed of a capacitive loop at a high-frequency region and an inductive impedance loop at a low-frequency region, indicating there were 2-time constants. Compared with that in a 3.5% NaCl solution without the inhibitor, the diameters of capacitive loops at a high-frequency region were larger when the Ce^{3+}-based inhibitor was added to a 3.5% NaCl solution, the charge-transfer resistance (R_t) is larger, showing that the corrosion rate of the low alloy steel in a 3.5% NaCl solution with the Ce^{3+}-based inhibitor decreased because of the effect of the Ce^{3+}-based inhibitor. Furthermore, the charge-transfer resistance increased with the immersed time. This may be due to that the effective compositions of the Ce^{3+}-based inhibitor were absorbed on the specimen surface with the immersed elapsed-time.

3.3.2 | Electrochemical parameters of interface electrochemical reaction

Generally, the capacitance element in electrochemical systems is represented by the constant-phase element (CPE) for fitting EIS spectra.[22]
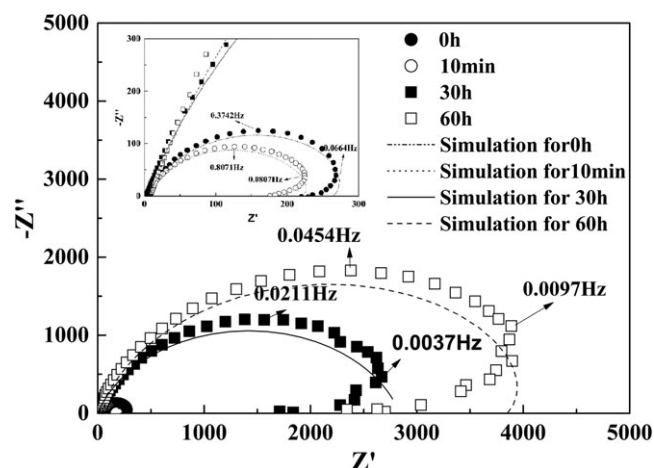

FIGURE 6 Nyquist plot of the low alloy steel in a 3.5% NaCl solution without and with the Ce^{3+}-based inhibitor for different times

The equivalent circuit used for fitting the EIS spectra shown in Figure 6 was presented in Figure 7, in which R_L is the solution impedance, Q is the constant-phase element, R_t is the charge-transfer resistance, R_0 is the equivalent resistance, and L is the inductive impedance. Based on the equivalent circuit, the EIS data were fitted by Simplex method, and the results were listed in Table 1.

As listed in Table 1, the charge-transfer resistance of electrode in a 3.5% NaCl solution without the inhibitor was 320.0 $\Omega.cm^{-2}$ and $\alpha < 1$, showing that the corrosion rate of the low alloy steel in a 3.5% NaCl solution was higher, and its surface properties were non-uniform.[22]

When the Ce^{3+}-based inhibitor was added to a 3.5% NaCl solution, the charge-transfer resistance of the electrode at the beginning of the immersion was 241.0 $\Omega.cm^{-2}$, which was smaller than that in a 3.5% NaCl solution without the inhibitor, showing the Ce^{3+}-based inhibitor accelerated the corrosion process of the low alloy steel electrode at the early immersed stage, and that the inhibitory film formed on the electrode surface through the corrosion process of the electrode in corrosive media.[23]

After the electrode was immersed in a 3.5% NaCl solution containing the inhibitor for more than 1.0 hours, electrochemical parameters were higher than that in a 3.5% NaCl solution without the inhibitor (Table 1). And that these electrochemical parameters increased with the immersed elapsed time, indicating that the inhibitory film containing Ce element retarded corrosion process. Therefore, the inhibitory efficiency of the Ce^{3+}-based inhibitor to the low alloy steel in a 3.5% NaCl solution increased with immersion time. Additionally, the increments of the equivalent resistance (R_0) and the inductive impedance (L) may imply that the inhibitory film on the electrode surface becomes more and more uniform and integrated. That is, if the electrode surface was wholly covered with the uniform and integrated inhibitory film, EIS spectra would have 1 time constant and that only would have a capacitive loop.
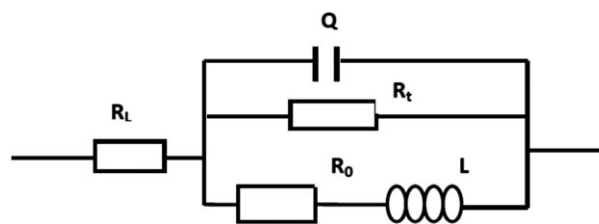

FIGURE 7 The equivalent circuit for fitting the EIS data presented in Figure 6

TABLE 1 Electrochemical parameters fitted with equivalent circuit based on EIS spectra of the low alloy steel in a 3.5% NaCl solution without and with the Ce^{3+}-based inhibitor for different times

Time, h	R_s, $\Omega.cm^2$	Q, $\Omega^{-1}.cm^{-2}.s^{\alpha}$	α	R_t, $\Omega.cm^2$	R_0, $\Omega.cm^2$	L, $H.cm^2$
0[a]	4.3	1.70×10^{-3}	0.81	320.0	772.9	3085.0
1/6	3.2	1.12×10^{-3}	0.80	241.0	1555.0	6502.0
30	2.1	8.25×10^{-3}	0.81	13 800.0	1421.0	441 400.0
60	3.6	7.80×10^{-3}	0.82	10 400.0	16 530.0	405 500.0

[a]In a 3.5% NaCl solution without the inhibitor.

It can be seen from Table 1 that the values of α did not change with immersion time and was equal to that without the inhibitor on the whole, demonstrating that the inhibitory film formed did not cover the whole surface, but it had better performances. It was clearly indicated that the Ce^{3+}-based inhibitor was mainly absorbed on the active sites, forming the net-shaped inhibitory film (Figure 1). Thus, the corrosion of the low alloy steel in a 3.5% NaCl solution was retarded with the Ce^{3+}-based inhibitor.

3.3.3 | Surface coverage of the inhibitory film

Based on the fitted electrochemical parameters listed in Table 1, the surface coverage of the electrode in a 3.5% NaCl solution containing the Ce^{3+}-based inhibitor can be calculated in accordance with the following equation[24]:

$$\gamma = \left(1 - \frac{C_{eff.ab}}{C_{eff.b}}\right) X 100\% \tag{1}$$

where, γ is the coverage rate, %; $C_{eff.\ b}$ and $C_{eff.\ ab}$ are the effective capacitance of the electrode immersed in a 3.5% NaCl solution without

TABLE 2 Effective capacitances and coverage rates of the low alloy steel in a 3.5% NaCl solution with the Ce^{3+}-based inhibitor for different times

Time, h	Ceff., μF.cm^{-2}	γ, %
0[a]	536.77	0.0
1/6	279.76	47.9
30	193.56	63.9
60	224.04	58.3

[a]In a 3.5% NaCl solution without the inhibitor.

and with the Ce^{3+}-based inhibitor, respectively. To calculate the effective capacitance of the electrode ($C_{eff.\ b}$, $C_{eff.\ ab}$), the following equation was used[25,26]:

$$C_{eff} = Q^{1/\alpha} \left(\frac{R_e R_t}{R_e + R_t}\right)^{(1-\alpha)/\alpha} \tag{2}$$

The results were listed in Table 2.

It was seen from Table 2 that the effective capacitance (C_{eff}) increased with immersion time; the surface coverage rate also increased with immersion time. However, it was only 60% or so, not up to 100%. This was further verified by SEM images (Figure 8).

As shown in Figure 8A, the polish traces on the specimen surface were clearly observed after the specimen had been immersed in a 3.5% NaCl solution containing the Ce^{3+}-based inhibitor for 5 minutes. At the same time, it was found that greyish products gathered at locally corroded sites. When specimen had been immersed for 1.0 hours, the polish traces were still clearly observed, and very small greyish product particles were also observed on the whole surface of the tested specimen (Figure 8B). Afterwards, the number of greyish product particles on the specimen surface increased with immersion time and that the sizes of these greyish product particles became larger and larger. Finally, as shown in Figure 8C,D, the net-shaped inhibitory film was formed on the specimen surface, and the polish traces on the specimen surface were still observed. Even if after the specimen was immersed in a 3.5% NaCl solution containing the Ce^{3+}-based inhibitor for 30.0 hours, the surface coverage was approximately 64.0%. The charge-transfer resistance (R_t) increased to 13 800.0 Ohm.cm^{-2}. The corrosion of the low alloy steel in a 3.5% NaCl solution containing the Ce^{3+}-based inhibitor was retarded. Therefore, the absorption
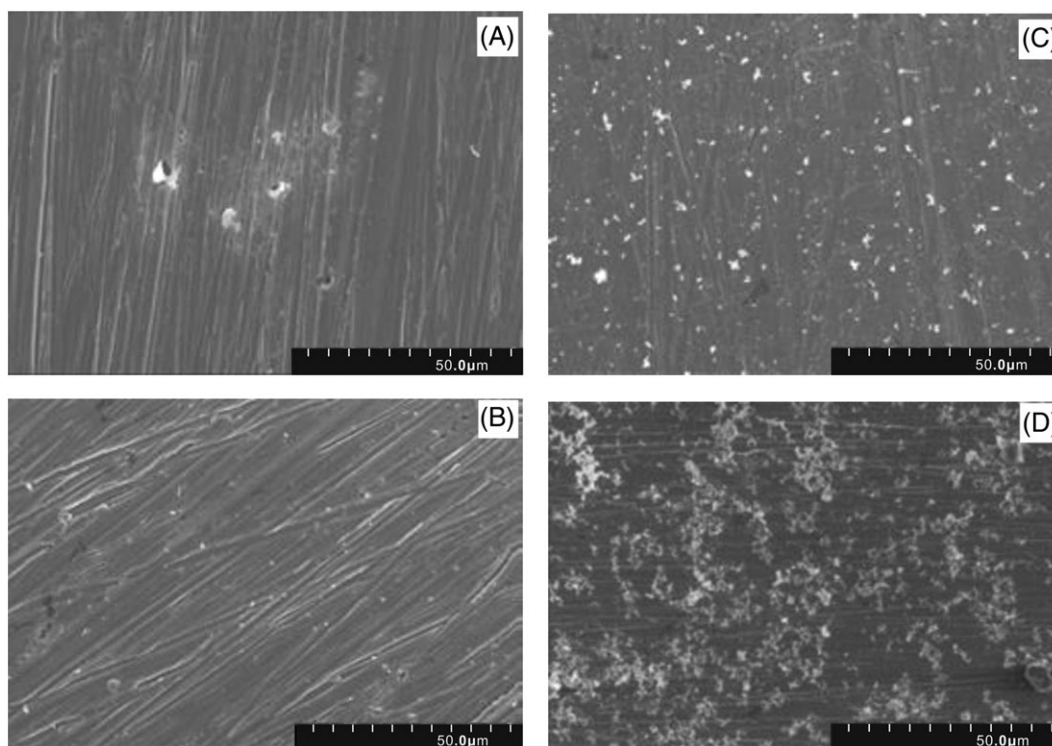

FIGURE 8 SEM images of specimens after immersed in a 3.5% NaCl solution containing the Ce^{3+}-based inhibitor for different times (A, 5 minutes; B, 1.0 hours; C, 10.0 hours; D, 30 hours)

effect mechanism of the Ce^{3+}-based inhibitor was further verified by SEM images.

3.3.4 | Kinetics of interface electrochemical reaction

Generally, when electrochemical processes are influenced by electrode potential and 1 state variable, its impedance (Z) of the equivalent circuit in Figure 7 can be expressed as[21,22]:

$$\frac{1}{Z} = \frac{1}{R_t} + \frac{A}{j\omega + B} \tag{3}$$

In Equation 4, $R_t > 0$, $B > 0$. And

$$A = m \cdot b \tag{4}$$

The Faraday current (I_F) of the electrode decreased with increasing the film thickness (δ) when the electrode was immersed in a 3.5% NaCl solution without the inhibitor. Thus, the following equation existed[23]:

$$m = \left(\frac{\partial I_F}{\partial \delta}\right)_{ss} < 0 \tag{5}$$

Pitting corrosion occurred on the surface of electrode because of the effect of Cl^- ions. Therefore, at the pitting sites, there was

$$b = \left(\frac{\partial \delta}{\partial \varphi}\right)_{ss} < 0 \tag{6}$$

Following Equations 5 and 6, $A > 0$. In this case, EIS spectra should have an inductive loop at a low-frequency region. This is consisted with Figure **6**, showing that the low alloy steel was subjected to pitting corrosion in a 3.5% NaCl solution.

When the Ce^{3+}-based inhibitor was added to the 3.5% NaCl solution, m represents the change of Faraday current (I_F) with the surface area (θ) covered with the inhibitory film under the stable condition and it can be expressed by Equation 7:

$$m = \left(\frac{\partial I_F}{\partial \delta}\right)_{ss} \tag{7}$$

Based on Equation 7, the Faraday current (I_F) decreases with the increase of the surface area (θ) covered with the inhibitory film, m < 0.

However, b means the change of the surface coverage (γ) of the inhibitory film with electrode potential (φ) under the stable condition, and it can be expressed by Equation 8.[21]
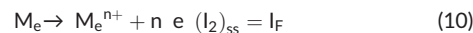
$$b = \left(\frac{\partial L}{\partial E}\right)_{ss} \tag{8}$$

where, $\gamma = \frac{d\theta}{dt}$.

Based on the absorption mechanism of the Ce^{3+}-based inhibitor, there occurred 2 chemical reactions on the electrode surface, which can be expressed as in the following:

$$M_e + A + e \overset{\leftarrow}{\rightarrow} (M_eA^-)_{ads} \qquad (I_1)_{ss} = 0 \tag{9}$$

$$1-\theta \quad \theta$$

$$M_e \rightarrow M_e^{n+} + n\ e \quad (I_2)_{ss} = I_F \tag{10}$$

$$1-\theta$$

where Me represents the metallic electrode. A is the Ce^{3+}-based inhibitor, which is absorbed on the electrode surface through the reaction 9. The reaction 9 occurs very fast. The corrosion reaction of the electrode only occurs on the un-covered surface with the Ce^{3+}-based inhibitor. In this case, the Faraday current density (I_F) is approximately equal to corrosion current density of the electrode. The electrode process is influenced by electrode potential and the surface area (θ) covered with the inhibitory film. Thus,

$$\gamma = \frac{d\theta}{dt} = K(I_{+1} - I_{-1}) \tag{11}$$

$$b = \left(\frac{\partial \gamma}{\partial \varphi}\right)_{ss} = -K\frac{F}{RT}[\alpha I_{+1} - (1-\alpha)I_{-1}] < 0 \tag{12}$$

where K is reaction constant. I_{+1} is the current density of the reaction 9 from left to right. I_{-1} is the current density of reversible reaction for the reaction 9.

Following Equations 7 and 12, Equation 4 can be expressed as

$$A = m \cdot b > 0 \tag{13}$$

Based on Equation 13, EIS spectra should have an inductive loop at a low-frequency region. This is also consisted with EIS spectra shown in Figure **6**.

3.4 | Interface reaction mechanism

Based on the previous results, the interface reaction model was established in Figure 9. As shown previously, pitting corrosion usually occurred on the surface of the low alloy steel in a 3.5% NaCl solution.[27,28] Corrosion reaction occurred: $Fe = Fe^{2+} + 2e$ and $O_2 + 2 H_2O + 4e = 4OH^-$, forming active sites on the surface of the low alloy steel. The active sites were called an anode zone; the balance areas were called a cathode zone. In this case, Fe^{2+} ions were concentrated in an anode zone and anions, such as OH^-, Cl^- contained in a 3.5% NaCl solution, including PO_4^{3-} and $P_2O_7^{4-}$ which were produced through the hydrolysis reaction of $P_3O_{10}^{5-}$, ie, $P_3O_{10}^{5-} + H_2O = PO_4^{3-} + H_2P_2O_7^{2-}$, moved over to anode zones. Thus, chlorides, hydroxides, and phosphates formed in anode zones, and finally the anode zones were covered, retarding the corrosion of the low alloy steel in a 3.5% NaCl solution. During this time, disproportionation reaction simultaneously occurred to Ce^{3+} ions, ie, $2Ce^{3+} = Ce^{2+} + Ce^{4+}$, forming Ce^{2+}, Ce^{4+} hydroxides, and phosphates on the surface of
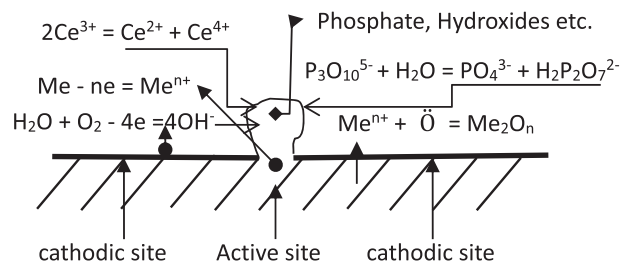

FIGURE 9 Scheme of interface reaction mechanism

the low alloy steel. Finally, the surface of low alloy steel in a 3.5% NaCl solution was covered with the net-shape inhibitory film with greyish product particles and that the low alloy steel was protected from corrosion.

4 | CONCLUSIONS

The Ce^{3+}-based inhibitor was an anodic inhibitor with the above 90.0% inhibitory efficiency, forming the net-shaped inhibitory film with nano-scale greyish product particles on the surface of the low alloy steel in a 3.5% NaCl solution.

Some complicated electrochemical and chemical reactions occurred at the interface between the surface of steel electrode and the 3.5% NaCl solution containing Ce^{3+}-based inhibitor, resulting in the movement of anions to active sites on the surface of the low alloy steel, and that the formation of the net-shape inhibitory film containing Ce element. Based on these reactions, the interface reaction model was established.

EIS spectra of the electrode in a 3.5% NaCl solution without inhibitor and with the Ce^{3+}-based inhibitor were composed of a capacitive loop at a high-frequency region and an inductive impedance loop at a low-frequency region. The former was induced by pitting corrosion on the electrode surface. The latter resulted from the formation and partial coverage of the net-shaped inhibitory film with nano-scale greyish product particles on the electrode surface.

ORCID

Xingyue Yong http://orcid.org/0000-0001-5547-2513

REFERENCES

1. Lin JC, Chang SL, LSL. Corrosion inhibition of steel by thiourea and cations under incomplete cathodic protection in a 3.5% NaCl solution and seawater. *J Appl Electrochem*. 1999;29(8):911-918.

2. Yang W, Kueiyuan H, Wang Q, Kong W. *Inhibitor*. Beijing: Chemical Industry Press; 1989:6.

3. Lin Y, Huanwen L, Masayoshi K. Inhibition effect of aluminum ion in combination with $C_2O_4^{2-}$ ion on corrosion of mild steel in water and its mechanism. *J Chin Society Corros protect*. 1992;12(1):56-61.

4. Oka Y, Ohkubo M. Mechanism of inhibitory effect on cavitation erosion-corrosion for iron in a 3% sodium chloride solution. *Corrosion*. 1990;46(8):687-695.

5. Meresht ES, Farahani TS, Neshati J. 2-Butyne-1, 4-diol as a novel corrosion inhibitor for API X65 steel pipeline in carbonate/bicarbonate solution. *Corros Sci*. 2012;54:36-44.

6. De Nicolo A, Paussa L, Gobessi A, AlexLanzutti CC, Andreatta F, Fedrizzi L. Cerium conversion coating and sol-gel multilayer system for corrosion protection of AA6060. *Surf Coat Technol*. 2016;287:33-43.

7. Valdez B, Kiyota S, Stoytcheva M, Zlatev R, Bastidas JM. Cerium-based conversion coatings to improve the corrosion resistance of aluminium alloy 6061-T6. *Corros Sci*. 2014;87:141-149.

8. Sherif EI-SM, Potgieter JH, Comins JD, Cornish L, Olubambi PA, Machio CN. The beneficial effect of Ruthenium additions on the passivation of duplex stainless steel corrosion in sodium chloride solution. *Corros Sci*. 2009;51(6):1364-1371.

9. Bin F, Koutsoukos P, Klepetsianis P, Forsyth M. The corrosion inhibition mechanism of new rare earth cinnamate compounds—electrochemical studies. *ElectrochimicaActa*. 2007;52:6212-6220.

10. Mishra AK, Balasubramaniam R. Corrosion inhibition of aluminium by rare earth chlorides. *Mater Chem Phys*. 2007;103(2-3):385-393.

11. Li X, Deng S, Fu H, Mu G. Synergism between rare earth cerium (IV) ion and vanillin on the corrosion of cold rolled steel in 1.0 M HCl solution. *Corros Sci*. 2008;50(12):3599-3609.

12. Laleh M, Kargar F, Sabour Rouhaghdam A. Investigation of rare earth sealing of porous micro-arc oxidation coating formed on AZ91D magnesium alloy. *J Rare Earths*. 2012;30(11):1293-1297.

13. Ivusic F, Lahodny-Sarc O, Curkovic HO, Alar V. Synergistic inhibition of carbon steel corrosion in seawater by cerium chloride and sodium gluconate. *Corros Sci*. 2015;98:88-97.

14. Yanhua Z, Jia Z, Yongsheng Y, Xianguang Z. Research on anti-corrosion property of rare earth inhibitor for X70 steel. *J Rare earths*. 2013;31(7):734-740.

15. Liu Y, Cheng YF. Inhibiting effect of cerium ions on corrosion of 3003 aluminum alloy in ethylene glycol-water solution. *J Appl Electrochem*. 2011;41:383-388.

16. Mishra AK, Balasubramaniam R. Corrosion inhibition of aluminum alloy AA 2014 by rare earth chlorides. *Corros Sci*. 2007;49(3):1027-1044.

17. Catubig R, Hughes AE, Cole IS, Hinton BRW, Forsyth M. The use of cerium and praseodymium mercaptoacetate as thoil-containing inhibitors for AA2024-T3. *Corros Sci*. 2014;81:45-53.

18. Muster TH, Sullivan H, Lau D, et al. A combinatorial matrix of rare earth chloride mixtures as corrosion inhibitors of AA 2024-T3: optimisation using potentiodynamic polarization and EIS. *Electrochim Acta*. 2012;67:95-103.

19. Aballe A, Bethencourt M, Botana FJ, Marcos M. $CeCl_3$ and $LaCl_3$ binary solution as environment-friendly corrosion inhibitors of AA 5083 al-mg alloy in NaCl solutions. *J Alloys Compd*. 2001;323-324:855-858.

20. Chunan C. *The Theory of Corrosion Electrochemistry*. Second ed. Beijing: Chemical Industry Press; 2004 p.234.

21. Chunan C, Jianqing Z. *An Introduction to Electrochemical Impedance Spectroscopy*. Beijing: Sciences Press; 2002:110.

22. Orazem ME, Tribollet B. *Electrochemical Impedance Spectroscopy*. NJ, USA: A John Wiley & Sons, Inc; 2008:120.

23. Chunan C. *The Principles of Corrosion Electrochemistry*. Beijing: Chemical Industry Press; 2004:150.

24. Nobial M, Devos O, Tribollet B. Electrochemical and in situ optical investigation of ZnO deposition. *J Cryst Growth*. 2011;327:173-181.

25. Brug GJ, Van Den Eeden ALG, Sluyters-Rehbach M, Sluyters JH. The analysis of electrode impedances complication by the presence of a constant phase element. *J Electroanal Chem*. 1984;176:275-295.

26. Hirschorn B, Mark EO, Tribollet B, Vivier V, Frateur I, Musiani M. Determination of effective capacitance and film thickness from constant-phase-element parameters. *Electrochim Acta*. 2010;55(21):6218-6227.

27. Shi J, Sun W, Jiang J, Zhang Y. Influence of chloride concentration and pre-passivation on the pitting corrosion resistance of low-alloy reinforcing steel in simulated concrete pore solution. *Construct Build Mater*. 2016;111(15):805-813.

28. Liu M, Cheng X, Li X, Lu T. Corrosion behavior of low-Cr steel rebars in alkaline solutions with different pH in the presence of chlorides. *J Electroanal Chem*. 2017;803(10):40-50.